

Electron spin resonance studies in β -FeSi₂ crystals

I. Aksenov, H. Katsumata, and Y. Makita
Electrotechnical Laboratory, Tsukuba, Ibaraki 305, Japan

Y. Kimura, T. Shinzato, and K. Sato
Tokyo University of Agriculture and Technology, Koganei, Tokyo 184, Japan

(Received 11 March 1996; accepted for publication 24 April 1996)

The electron spin resonance studies have been carried out in the temperature range 130–300 K on semiconducting β -FeSi₂ single crystals grown by a chemical vapor transport technique. Two anisotropic doublets with apparent g factors in the range 2.025–2.05 and 1.98–2.03, as well as one complex signal having an isotropic g factor of 2.0195 and exhibiting a five-line hyperfine structure, have been detected. The doublet signals are believed to arise from spin triplet ($S=1$) states of, presumably, substitutional Ni²⁺ transition ions, whereas the signal exhibiting the hyperfine structure has been attributed to the spin of a hole, captured by silicon vacancy and interacting with nuclear spins of four iron atoms in the first shell surrounding of the silicon vacancy. © 1996 American Institute of Physics. [S0021-8979(96)04115-1]

I. INTRODUCTION

Silicides form an interesting and important group of compounds compatible with state-of-the-art semiconductor technology. While the majority of the silicides turn out to be metallic, some of them, including the orthorhombic β phase of iron disilicide (β -FeSi₂), have been found to exhibit semiconducting properties.¹ Due to its direct band gap² (e.g., ~0.83–0.89 eV), as well as relatively high values of the Hall mobilities for electrons and holes^{3,4} ($\mu_n \sim 50$ cm²/V s and $\mu_p \sim 1200$ cm²/V s), β -FeSi₂ has been receiving considerable attention as a very promising material for Si-based photovoltaic and optoelectronics applications. Moreover, the β phase of FeSi₂, like all iron silicides, exhibits high resistance to oxidation, lack of toxicity, low vapor pressure, as well as an abundance of constituent elements in the Earth crust, the above properties being also attractive for semiconductor technology.

However, there are some important problems to be solved before β -FeSi₂ can be efficiently used as an electronic material, those problems being: (1) the difficulty of β -FeSi₂ preparation due to complexity of the iron–silicon phase diagram showing that iron and silicon form four compounds, Fe₂Si, Fe₆Si₃, ϵ -FeSi, α -Fe₂Si₅, and β -FeSi₂, among which only FeSi and β -FeSi₂ are thermodynamically stable at room temperature (RT);⁵ (2) the mainly (Fe)*d* character of the band edge states in β -FeSi₂ resulting in flat valence-band-maximum and conduction-band-minimum states,⁶ so that the deformation potential, produced by localized states in the crystal lattice, is strong enough to alter the energy gap and probably, even its nature;⁷ and (3) the dimensions of the orthorhombic cell⁸ ($a=9.86$ Å, $b=7.79$ Å, $c=7.83$ Å) in which β -FeSi₂ crystallizes provide a bad match with silicon, resulting in misfit dislocations at the FeSi₂/Si interface and in the appearance of different domains in the epitaxial films and, therefore, in the bad crystalline quality of the films.⁹

As a result of the above problems, most of the previous measurements of the properties of β -FeSi₂ have been carried out on sintered samples or on polycrystalline films. Those data, however, are either unreliable or difficult to interpret

due to the effects of the substrate, interface, grain size, and structure, which are difficult to evaluate.

Single crystals of β -FeSi₂ have been prepared, only recently and by only one research group, by chemical vapor transport (CVT) and used for electronic transport and photoconductivity measurements, resulting in the observation of several defect centers with activation energies of ~70 meV (donorlike defect), as well as ~55 meV and ~100–120 meV (acceptorlike defects).^{3,4,10} The nature of these defect centers, however, has not been elucidated even tentatively.

We, therefore, used the powerful method of electron spin resonance (ESR) to probe the nature of defects in undoped β -FeSi₂ single crystals grown by the CVT technique. Two anisotropic doublets presumably arising from the $S=1$ states of the divalent nickel ions, as well as a signal from a hole captured by a silicon vacancy, have been detected.

II. CRYSTAL GROWTH AND EXPERIMENT

The crystals were grown by CVT using iodine as a transporting agent from the commercially available FeSi₂ powder. About 7 g of the powder together with iodine concentration of about 7 mg/cm³ were sealed in an evacuated (10⁻⁶ Torr) quartz ampoule of 18 mm inner diam and 200 mm in length, the ampoule then being placed in the two-zone electrical furnace. Two temperature profiles have been used for the growth with the temperatures of the growth zone T_g and source zone T_s being shown in Table I together with the temperature gradient ΔT_{sg} . It can be seen that the temperature of the growth zone was kept constant while that of the source zone was gradually raised so that the temperature gradient was changing from -30 °C (growth zone cleaning mode) up to 250 °C (growth No. 1) or 200 °C (growth No. 2) during 14 days.

The CVT technique yielded the samples of (1) the homogeneous β -FeSi₂ phase, as well as (2) the α -Fe₂Si₅ phase with a small admixture of the ϵ -FeSi phase, i.e. ($\alpha+\epsilon$) phase, which is in accordance with the phase diagram of the Fe–Si system.⁵ The metallic ($\alpha+\epsilon$)-phase samples formed in the middle of the ampoule where the temperature was high

TABLE I. The temperature profile parameters for the CVT growth together with resulting crystals and their composition determined by electron probe microanalysis (EPMA) using a JEOL microanalyzer with an electron acceleration voltage of 15 kV.

Growth run	T_g (°C)	T_i (°C)	ΔT_{ig} (°C)	Obtained phases	Composition (EPMA)
No. 1	750	720 \Rightarrow 1000	-30 \Rightarrow 250	($\alpha + \epsilon$) β	Fe ₂ Si _{1.3} FeSi _{2.06}
No. 2	800	770 \Rightarrow 1000	-30 \Rightarrow 200	($\alpha + \epsilon$) β	Fe ₂ Si _{1.1} FeSi _{1.94}

enough for the formation of the high-temperature α phase of FeSi₂, whereas the crystals of the low-temperature β -FeSi₂ grew closer to the growth zone of the ampoule where the temperature was below the temperature of the $\alpha \Rightarrow \beta$ phase transition $T_{\alpha\beta} = 937$ °C.⁵ Silicon was found to condense at the colder part of the ampoule so that crystals grew on the deposited layer of silicon.

The crystals of the ($\alpha + \epsilon$) phase were typically plate shaped with dimensions of about 2×2 mm² and exhibited low resistivity values of about 10^{-3} Ω cm (the phase is metallic), whereas the crystals of the orthorhombic β -FeSi₂ phase grew predominantly in the form of thin needles of about 10 mm in length and showed resistivities of the order 10^2 Ω cm. The above results are similar to those reported by Kloc *et al.*¹⁰ It can also be seen from Table I that the growth process No. 1 resulted in Si-rich β -FeSi₂ crystals, whereas the growth process No. 2 yielded Si-deficient samples of the β phase.

The crystals of β -FeSi₂ were then used for the ESR measurements, which were carried out with a JEOL X-band spectrometer in the temperature range 130–300 K with the microwave power being 5 mW. The ESR spectra were taken on nonoriented crystals, and it turned out that the spectra are different for the Si-rich and Si-deficient samples (obtained by the growth process No. 1 and No. 2, respectively) as discussed below.

III. ESR RESULTS AND DISCUSSION

A. Anisotropic signals

Figure 1 shows the ESR spectra of the Si-rich (upper trace) and Si-deficient (lower trace) β -FeSi₂ crystals. Four absorptions, marked as A_1 , A_2 , B_1 , and B_2 , were detected in both Si-rich and Si-deficient samples. The measurements of the temperature dependence of the intensities of these absorptions revealed that the intensities of a set of two A_i signals ($i=1,2$) changed simultaneously with temperature, the same behavior being observed for a set of two B_i signals. At the same time, the thermal quenching of the A_i signals was different from that of the B_i signals, the set of A_i signals being quenched much faster with increasing temperature than the set of B_i signals. We, therefore, believe that the A_i and B_i signals originate from different centers.

Both A_i and B_i signals are anisotropic doublets, and the spectral positions of their "centers of gravity" change depending on the orientation of the crystals in the range of apparent g factors $g_A = 2.025$ – 2.05 and $g_B = 1.98$ – 2.03 for A_i and B_i signals, respectively. The splitting between two sig-

nals in each of the A_i and B_i doublets is anisotropic (about 0.7–1.4 mT depending on the orientation of the samples), and the relative intensities of the signals within A_i and B_i doublets also vary with the crystal orientation. We, therefore believe that both A_i and B_i doublets arise from some crystal defects the ground state of which is a spin triplet ($S=3$), slightly (of the order of 1 mT $\sim 5 \times 10^{-4}$ cm⁻¹) split by the effect of a noncubic ligand field at the sites of these defects.

Considering the orthorhombic crystal structure of β -FeSi₂, which can be viewed as a distorted fluorite (CaF₂- γ) structure,¹¹ we can see that each silicon atom in the β -FeSi₂ crystal lattice has four iron neighbors, the local symmetry at the Si site being the distorted T_d ; whereas each iron atom is surrounded by eight silicon atoms in the first shell, the local symmetry at the Fe site being the distorted O_h . Therefore, the transition metal ions V^{3+} or Ni^{2+} of the iron group with d^2 - or d^8 -electronic configuration ($S=1$), respectively, substituting for either Si or Fe sites in the lattice, may give rise to the observed ESR doublet signals.¹²

The chemical analysis of our samples revealed the presence of nickel impurity in high concentrations (≈ 200 ppm), whereas no vanadium has been detected. Therefore, we tentatively attribute the observed fine structures A_i and/or B_i to the substitutional Ni^{2+} occupying iron and/or silicon sites in the crystal lattice. A lack of the knowledge of the exact orientation of the samples in relation to the external magnetic

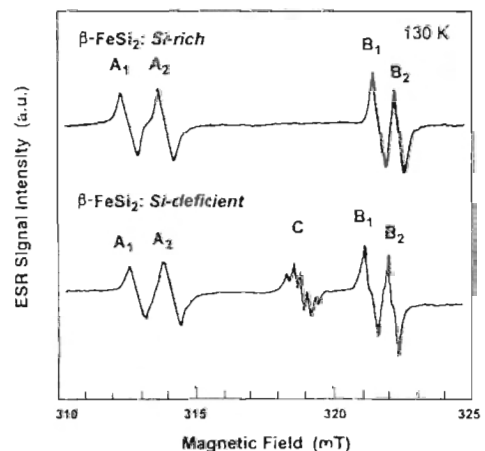


FIG. 1. The typical ESR spectra of the β -FeSi₂ crystals taken at 130 K. No other signals were detected in the magnetic field range 0–800 mT.

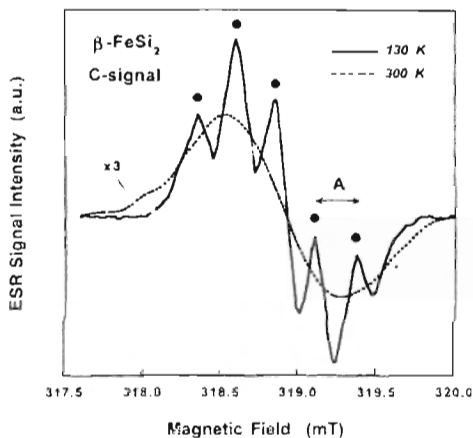


FIG. 2. The detailed spectrum of the C signal taken at 130 K and at room temperature. The sharp lines are due to the ligand hyperfine interaction, and the energy separations between the lines equal to the hyperfine splitting parameter $A = (1.0\text{--}1.3) \times 10^{-4} \text{ cm}^{-1}$.

field precluded, however, any estimations of the spin Hamiltonian parameters for the above centers.

B. Isotropic signal due to silicon vacancy

As can be seen from Fig. 1, the Si-deficient samples (but not the Si-rich ones) exhibit, in addition to the above discussed A_i and B_i signals, also a rather complex C signal consisting of five sharp (peak-to-peak width $\Delta H_{pp} \approx 0.5 \times 10^{-4} \text{ cm}^{-1}$) equidistant lines superposed on a broader signal with $\Delta H_{pp} \approx 3 \times 10^{-4} \text{ cm}^{-1}$ and centered at $g = 2.0195 \pm 0.001$. The g factor of the C signal is isotropic within the experimental error of our measurements (± 0.001), and the energy separation between the five sharp lines (marked as "A" in Fig. 2) changes slightly upon rotation of the sample within the range $(1.0\text{--}1.3) \times 10^{-4} \text{ cm}^{-1}$.

Figure 2 shows the detailed spectrum of the C signal at 130 K (thick trace) and RT (thin dashed curve). The peak-to-peak intensities of the five lines are in the ratio of 1.0:3.6:5.5:3.5:0.9. It can also be seen that at RT the five-line structure disappears, and some thermal broadening of the background signal occurs due to an increased interaction of the spin system with phonons.

We were surprised, at first, to observe the isotropic signal from $\beta\text{-FeSi}_2$ exhibiting a fairly low (orthorhombic) symmetry. A close look at the structure of $\beta\text{-FeSi}_2$ and comparison of it with that of the cubic CaF_2 structure (space group O_h^F), however, reveals that while the eight-fold cubic coordination of Si atoms around Fe ones is greatly distorted in $\beta\text{-FeSi}_2$ in comparison with CaF_2 , the four-fold tetrahedral coordination of Fe atoms around Si ones is essentially preserved, except for a slight (about 2.2%) expansion of the Fe-Si bond length.⁸ Due to the above considerations, and since the g factor of the C signal is larger than that of a free electron $g_0 = 2.0023$, we believe that the C signal originates from a hole ($S = 1/2$) trapped on a silicon vacancy V_{Si} and equally shared by the four nearest Fe atoms of the first shell

surrounding of V_{Si} . The assignment of the C signal to the V_{Si} defect is supported by the fact that the C signal has been observed only in the Si-deficient samples, and not in the Si-rich ones.

The electronic structure of the V_{Si} defect may be described considering that when the Si site is vacant, there are four dangling bond orbitals from the nearest Fe atoms. We can construct molecular orbitals from these dangling bonds, and in T_d symmetry the resulting orbitals will consist of a singlet level A_1 and a triply degenerate level T_2 .¹³ The triplet T_2 is further split into three singlets by the effect of the low-symmetry component of the crystal field in $\beta\text{-FeSi}_2$. Therefore, trapping of the hole by a neutral silicon vacancy V_{Si}^0 having four electrons and the total spin $S_i = 0$ will result in a V_{Si}^+ defect with $S_i = 1/2$. The microwave transitions $-1/2 \rightleftharpoons 1/2$ will then result in the observed C signal. The expected small anisotropy of the C signal due to the low symmetry of the second- and third-shell surroundings of the silicon vacancy may be greatly reduced by a thermally stimulated hopping of the hole between four Fe atoms, which results in the detection of an averaged spectrum.¹⁴

Furthermore, the observed five-line structure can be unambiguously assigned to the (super)-hyperfine interaction of the spin of the hole on V_{Si} with four neighboring nuclear spins $I = 1/2$ of ^{57}Fe nuclei. Since the total nuclear spin of four ^{57}Fe nuclei is $I_i = 4 \times I = 2$, we can expect $2 \times I_i + 1 = 5$ lines of the ligand hyperfine structure, which is in complete agreement with our experimental results. Since the content of ^{57}Fe isotope with $I = 1/2$ is only 2.2% and the other Fe isotopes have $I = 0$, the ligand hyperfine structure lines are observed as being superposed on a broader background signal. Moreover, depending on the number of possible combinations of the quantum number m_I to form the total quantum number M_I , the transitions for $I = 1/2$ and four equivalent Fe nuclei should have the statistical weights as 1:4:6:4:1 for $M_I = 2, 1, 0, -1, -2$, respectively, which is very close to the observed intensities ratio of the hyperfine structure components 1.0:3.6:5.5:3.5:0.9.

We, therefore, can definitely assign the C signal as originating from the hole trapped at a silicon vacancy and equally shared by four nearest Fe atoms in the crystal lattice, the hyperfine interaction of the hole spin with spins of Fe nuclei resulting in the slightly anisotropic ligand hyperfine structure with the hyperfine interaction parameter $A = (1.0\text{--}1.3) \times 10^{-4} \text{ cm}^{-1}$.

The temperature dependence of the intensity of the C signal is shown in Fig. 3, from which we can deduce the activation energy of the thermal emission of captured holes from the V_{Si} defect. If an energy level, formed by some defect in the band gap of a semiconductor, is "shallow" enough, then we can use the Hartree-Fock approximation stating that an empty electronic state of the defect (V_{Si}^0 , in our case) and its filled state (V_{Si}^+ , in our case) can be characterized by the same energy level, the ionization energy of which can be deduced from the thermal quenching curve reflecting the process of the thermal emission of captured carriers (holes, in our case) from the defect level. From the principle of the detailed balance, the intensity of the C sig-

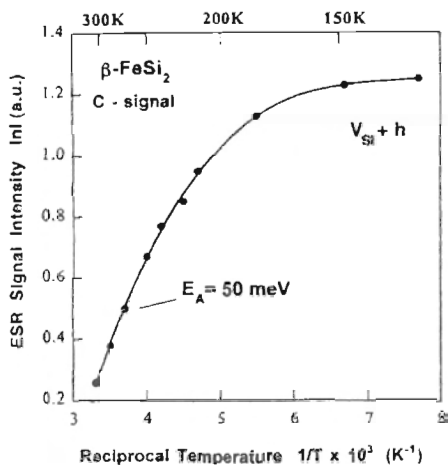


FIG. 3. Thermal quenching curve for the C signal. The contribution from the sharp hyperfine structure was deducted when calculating the intensity of the C signal.

nal, formed by holes still captured on V_{Si} defects, can be written as

$$I(T) = I_0 [-f(T) \exp(-E_A/kT)], \quad (1)$$

where $f(T)$ is a slow (as compared with exponential) function of temperature and I_0 is the intensity of the C signal at $T \rightarrow 0$. Neglecting $f(T)$ we, therefore, can determine the value of the ionization energy E_A from the slope of $\ln I$ vs $1/T$, which results in the activation energy of V_{Si} defect: $E_A = 50 \pm 10$ meV as shown in Fig. 3. It should be noted that this activation energy agrees well with that of the acceptor ($E'_A = 55$ meV) detected previously in β -FeSi₂ from the electronic transport measurements. The silicon vacancies, therefore, may be influencing the electrical properties of β -FeSi₂.

IV. CONCLUSIONS

The ESR studies of the orthorhombic β -FeSi₂ crystals revealed (1) two anisotropic signals with apparent g factors

in the range 2.025–2.05 and 1.98–2.03, presumably originating from the fine structure transitions within the ground triplet ($S=1$) states of substitutional Ni^{2+} transitions metal ions, as well as (2) one complex signal exhibiting an isotropic g factor of 2.0195 and a five-line hyperfine structure, arising from the hyperfine interaction between the spin of a hole, captured by a silicon vacancy, and nuclear spins of four iron atoms in the first shell surrounding of the silicon vacancy. The activation energy of the acceptor state, formed by the silicon vacancy, was estimated as $E_A = 50 \pm 10$ meV from the thermal quenching curve of the ESR signal.

ACKNOWLEDGMENT

One of the authors (I. Aksenov) would like to thank the Science and Technology Agency of Japan for financial support.

- ¹J. Derrien, in *Properties of Metal Silicides*, edited by K. Maex and M. V. Rossum (INSPEC, London, 1995), p. 155.
- ²M. C. Bost and J. E. Mahan, *J. Appl. Phys.* **64**, 2034 (1988).
- ³E. Arushanov, Ch. Kloc, and E. Bucher, *Phys. Rev. B* **50**, 2653 (1994).
- ⁴E. Arushanov, Ch. Kloc, H. Hohl, and E. Bucher, *J. Appl. Phys.* **75**, 5106 (1994).
- ⁵O. Kubaschewski, in *Iron-Binary Phase Diagrams* (Springer, Berlin, 1982), p. 136.
- ⁶N. E. Christensen, *Phys. Rev. B* **42**, 7148 (1990).
- ⁷C. H. Oik, S. M. Yalisove, and G. L. Doll, *Phys. Rev. B* **52**, 1692 (1995).
- ⁸Y. Dusausoy, J. Protas, R. Wandji, and B. Roques, *Acta Crystallogr. Sect. B* **27**, 1209 (1971).
- ⁹A. Rizza, B. N. E. Rosen, D. Freundt, Ch. Dieker, H. Luth, and D. Gerthsen, *Phys. Rev. B* **51**, 17 780 (1994).
- ¹⁰Ch. Kloc, E. Arushanov, M. Wendl, H. Hohl, U. Malang, and E. Bucher, *J. Alloys Comp.* **219**, 93 (1995).
- ¹¹L. Miglio and G. Majori, *Phys. Rev.* **52**, 1448 (1995).
- ¹²A. Abragam and B. Bleaney, *Electron Paramagnetic Resonance of Transition Ions* (Dover, New York, 1986), p. 469.
- ¹³A. M. Stoneham, *Theory of Defects in Solids* (Clarendon, Oxford, 1975), p. 853.
- ¹⁴H. J. Bankeleben, A. Goltzwe, and C. Schwab, *Phys. Status Solidi B* **76**, 363 (1976).